Novel Reversible Ionic-to-Covalent Transition in a Highly Conducting TTF Derivative

Clifton Kwang-Fu Shen, Hieu M. Duong, Gursel Sonmez, and Fred Wudl*

Department of Chemistry and Biochemistry and Exotic Materials Institute, University of California at Los Angeles, Los Angeles, California 90095-1569

Received July 29, 2003; E-mail: wudl@chem.ucla.edu

While there are numerous reports, as recent as this year, on the very interesting consequences of the neutral-to-ionic transition in tetrathiafulvalene-chloranil (TTF-CA),[1] there are no reports on the solid-state properties of tetrathiafulvalene-*o*-chloranil (TTF-*o*-CA). Since it is well-known that *o*-chloranil is a stronger electron acceptor than its para isomer,[2] we decided to take a closer look. As we describe within, we discovered a novel reactivity of TTF.

When a solution of TTF is treated with a solution of *o*-chloranil in anhydrous acetonitrile at room temperature, not unexpectedly, there is an instantaneous formation of a brown-black solution, followed by slow precipitation of a black powder (**3**, Scheme 1). If the solution is allowed to stir for longer than 10 min, it very slowly bleaches, and white crystals (**4**, Scheme 1) are obtained along with black precipitate **3**. Electrospray ionization (ESI) mass spectrometric study using neutral effluent (pure CH$_3$CN), to prevent protonation or charge transfer from carrier solvent to target molecules, was performed in both positive and negative ion detection mode. As expected, there was no signal recorded in either positive or negative mode when a solution of **4** in acetonitrile was injected. In contrast, **3** showed a strong signal at *m/z* 203.8, which defined it as the parent TTF in positive mode. The parent pyrocatechol radical anion (M$^-$ *m/z* 246.7) and **4** ((M − H)$^-$ *m/z* 448.6) were found in negative mode (see Supporting Information). We surmised, correctly it turned out, that compound **4** was a cycloadduct. Single-crystal X-ray crystallography revealed a benzodioxane structure[3] shown in Scheme 1. Interestingly there are two slightly different conformers in the solid state (see Supporting Information).

The reaction progress in Scheme 1 can be easily monitored by UV−vis spectroscopy. A titration experiment, shown in Figure 1, demonstrates that an increase in the intensity of the UV−vis spectra arising from **3** and **4** and a decrease of TTF absorption, undoubtedly support formation of charge-transfer salt **3** and cycloadduct **4** in solution. The two broad visible absorption peaks between 400 and 650 nm correspond to the absorptions of TTF radical cation, which was further confirmed by in situ spectroelectrochemistry of TTF to afford the same species.

The dark solution, as well as the dark brown powder of **3**, exhibited a strong ESR signal with a solution *g*-shift value of 2.0081 (cf. for TTFCl *g* = 2.0083).[4−6] The hyperfine spectrum of a solution sample (Figure 2), provided further confirmation for the TTF radical cation in solution. The presence of the *o*-CA$^{•−}$ is observed only indirectly by its effect on the TTF$^{•+}$ signal through the slight broadening of the lines and negative shift of the *g* value (0.0009). The absence of a signal due to *o*-CA$^{•−}$ is very likely due to the lack of C−H bonds and low natural abundance of ^{17}O.

The compressed pellet conductivity of **3** was ca. 10^{-2} S/cm, implying that the single-crystal conductivity is expected to be ca. 1 S/cm, considerably higher than TTF-*p*-chloranil (10^{-5}−10^{-6} S/cm).[4] The combined results of ESR, conductivity, and elemental analysis strongly suggest that the structure of this particular radical

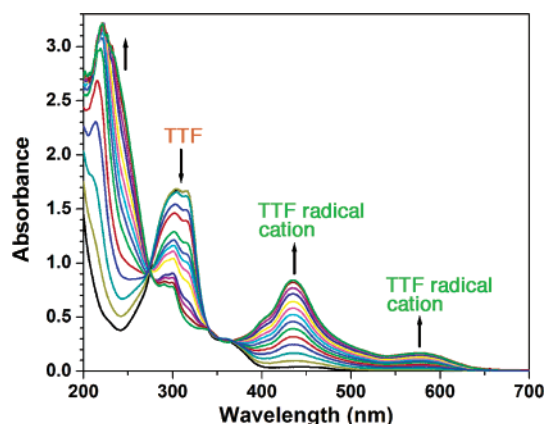**Figure 1.** UV−vis absorption spectrum of titration of **1** (10^{-4} M) with **2** (8.9 × 10^{-3} M) in CH$_3$CN.
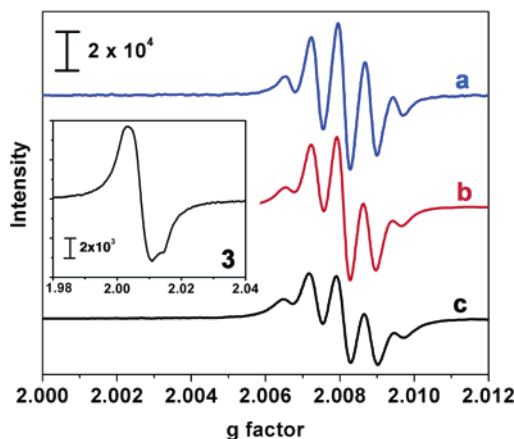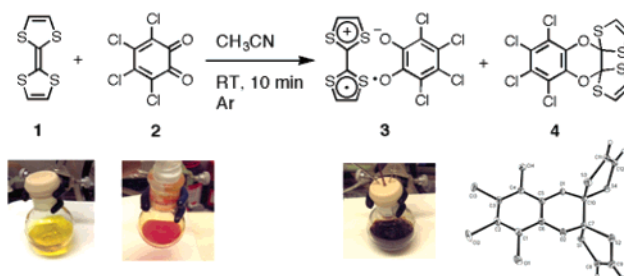

Figure 2. ESR spectra of (a) **3** in CH$_3$CN; (b) TTF$^{•+}$ (generated by bleach oxidation) of TTF in CH$_3$CN; (c) radical cation of **1** (generated by heating **4** under Ar at 155 °C) in CH$_3$CN, **3** in solid state (insert diagram).

Scheme 1. Synthetic Scheme of TTF-*o*-chloranil Complexes

ion salt is that of a traditional organic metal, i.e. segregated, partially charged stacks of TTF and *o*-CA. In addition, the spin density of **3** was determined to be ca. 33% vs DPPH. Unfortunately, we have
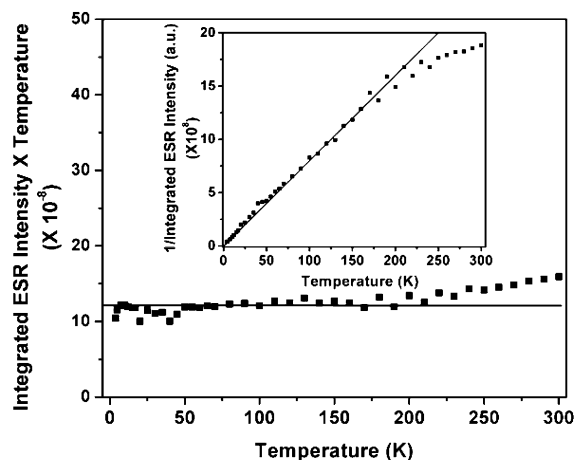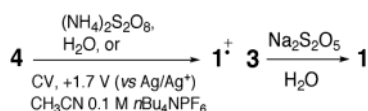
Figure 3. Solid-state variable-temperature ESR data of **3**.

Scheme 2. Interconversion of **3** and **4** to TTF and TTF Radical Cation

not been able to grow a sufficiently large crystal for X-ray structure determination, and powder XRD was uninformative because very few lines were observable over a large amorphous background.

Variable-temperature ESR measurements were carried out on powdered samples of **3**. The temperature dependence of the doubly integrated ESR signal, proportional to magnetic susceptibility, shows normal Curie–Weiss behavior between 230 and 4 K. The effective moment $[(\chi)(T)$ vs $T]$ plot (Figure 3, main plot) further confirms this observation. In these plots, the straight lines are a guide for the eye, indicating that within experimental error the effective moment is temperature independent between 230 and 4 K.[7]

The conversion of **4** back to TTF radical cation is possible either thermally or chemically. Heating a sample of **4** in the ESR cavity under Ar to 155 °C converted it from an ESR silent material to one exhibiting a strong signal with a solution g-value essentially equivalent to that of **1**$^{\bullet+}$ (2.0070 vs 2.0078).[5,6] Treatment of a solution of **4** with sodium peroxydisulfate also produced **1**$^{\bullet+}$ cleanly, as determined in a spectroscopic titration (see Supporting Information). In a similar fashion, the radical ion salt **3** can also be reduced back to neutral TTF **1** by aqueous $Na_2S_2O_5$ solution (Scheme 2).

When the cyclic voltammetry of **4** was recorded between 0 and 1.5 V vs Ag/Ag$^+$ in 0.1 M n-Bu$_4$NPF$_6$/CH$_3$CN, two redox waves were observed at 0.35 and 0.8 V (low current black curve in Figure 4). As the potential window was extended to 2.5 V, an irreversible oxidation was observed at ca. 1.9 V, likely due to the oxidative decomposition of **4**. In the following cycles, a dramatic increase in the intensity of the redox waves at 0.35 and 0.8 was observed (red curve, Figure 4), supporting the reversion of **4** leading to TTF and o-chloranil. The resulting TTF produced by electrochemical degradation can be reversibly oxidized and reduced several times. By keeping the potential at 1.7 V for 30 min, the solution color changed from colorless to dark brown, indicating the production of TTF$^{\bullet+}$ in accord with data from the UV–vis titration experiment (above).[8]
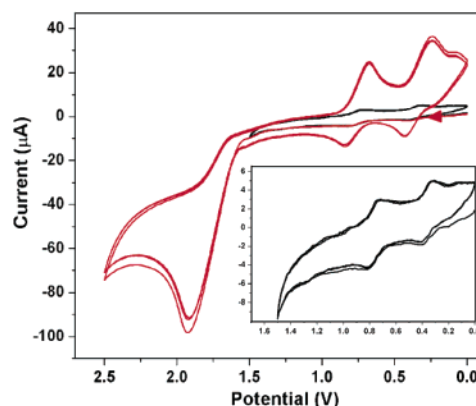

Figure 4. Cyclic voltammogram of **4** in CH$_3$CN. First six cycles between 0 and 1.5 V (low current black line and insert); second six cycles between 0 and 2.5 V (red line).

In summary, TTF produces two completely different phenomena with the different isomers of chloranil; with the para isomer it produces an insulating, alternating stack, ambient temperature neutral solid. While with the ortho isomer, it produces a more interesting system consisting of interconvertible conducting ionic and **covalent** components.

Supporting Information Available: Detailed descriptions of synthetic method, UV–vis spectra for titration experiment, ESI-MS data, and IR spectra (PDF). X-ray crystallography data in CIF format. This material is available free of charge via the Internet at http://pubs.acs.org.

References

(1) (a) Collet, E.; Lemée-Cailleau M.-H.; Cointe M. B.-L.; Cailleau H.; Wulff, M.; Luty, T.; Koshihara, S.-Y.; Meyer, M.; Toupet, L.; Rabiller, P.; Techert, S. *Science* **2003**, *300*, 612. (b) Cointe, M. L.; Lemée-Cailleau, M. H.; Cailleau, H.; Toudic B.; Toupet, L.; Heger, G.; Moussa, F.; Schweiss, P.; Kraft, K. H.; Karl, N. *Phys. Rev. B* **1995**, *51(6)*, 3374. (c) Horiuchi, S.; Kumai, R. *J. Am. Chem. Soc.* **1998**, *120*, 7379. (d) Aoki, S.; Nakayama, T.; Miura, A. *Synth. Met.* **1995**, *70*, 1243.
(2) (a) Sawyer, D. T.; Sobkowiak, A.; Roberts, J. L., Jr. *Electrochemistry for Chemists*; Wiley: New York, 1995; Chapter 12. (b) Lomprey, J. R.; Guarr, T. F.; Baumann, K. L. U.S. Patent 6,433, 914, 2002.
(3) Crystal data and structure information: (a) Crystal system: triclinic. (b) Space group: P-1 (c) Unit cell dimension: $a = 11.515(1)$ Å, $\alpha = 79.635(1)°$; $b = 12.746(1)$ Å, $\beta = 76.811(1)°$; $c = 13.022(1)$ Å, $\gamma = 89.147(1)°$. (d) $Z = 4$. (e) Goodness-of-fit on F^2: 1.029 (f) R indices (all data): R1 = 0.0268, wR2 = 0.058.
(4) Wudl, F.; Smith, G. M.; Hufnagel, E. J. *J. Chem. Soc., Chem. Commun.* **1970**, 1453.
(5) (a) Wudl, F.; Wobschall, D.; Hunfnagel, E. J. *J. Am. Chem. Soc.* **1972**, *94*, 670. (b) Torrance, J. B.; Mayerle, J. J.; Lee, V. Y.; Bechgaard, K. *J. Am. Chem. Soc.* **1979**, *101*, 4748. (c) Mitani, T.; Kaneko, Y.; Tanuma, S.; Tokura, Y.; Koda, T.; Saito, G. *Phys. Rev. B* **1987**, *35(1)*, 427.
(6) All g values of ESR spectra reported here have been calibrated by DPPH (diphenylpicrihydrazyl).
(7) There appears to be a hint of antiferromagnetic ordering between 300 and 230 K which will be examined by SQUID magnetometry.
(8) See Figure 3 in Supporting Information.

JA037621N